International Journal of Fluid Power 10 (2009) No. 1 pp. 47-57

FINITE ELEMENT ANALYSIS OF 3D VISCID PERIODIC WAVE PROPAGATION IN HYDRAULIC SYSTEMS

Rudolf Scheidl, Bernhard Manhartsgruber and Mohamed Ez El Din

Johannes Kepler University Linz, Institute of Machine Design and Hydraulic Drives, Altenbergerstr. 69, 4040 Linz, Austria
rudolf.scheidl@jku.at, bernhard.manhartsgruber@jku.at

Abstract

A very compact description of viscid wave propagation in straight transmission lines with a circular cross section in frequency domain by a transcendental transfer matrix is known since several decades. The corresponding research results show that fluid friction is limited to small dynamic boundary layers whereas the remaining fluid domain exhibits practically no friction effect and has bulk flow characteristics. An explanation how this boundary layer transfers its dissipative effect to the bulk flow has been given by Gittler et al. using asymptotic expansion techniques. They found that the effect of the boundary layer on the bulk flow in the centre is given by radial velocity components. The authors have shown that the findings of Gittler et al. are generally valid in the 3D case exploiting matched asymptotic expansions.

In this paper these results are developed further to exploit this dynamical boundary layer theory for an efficient Finite Element (FE) computation of viscid waves. Standard acoustic elements without viscosity as available in many FE codes combined with frequency dependent acoustic boundary conditions can be used to simulate 3D viscid wave propagation in frequency domain. Comparison with the analytical transmission line theory shows the validity and wide applicability of this approach. It is much more efficient than a direct resolution of the viscid boundary layer by a fine FE grid.

Keywords: 3D viscid wave propagation, finite element analysis, singular perturbation, boundary layer theory

1 Introduction

In hydraulics, wave propagation effects play a significant role mostly only in transmission lines, since the geometrical extensions of other fluid ducts are much smaller than typical wave lengths. Numerous mathematical models have been developed to study wave propagation processes in nearly straight transmission lines of circular cross section. Stecki (1986) gives an overview until 1986. Often, the effects of fluid friction on the dynamics of the system – which result in a frequency dependent damping – have to be modelled quite accurately. A very compact description of waves in transmission lines considering viscosity is given in the frequency domain (D'Souza, 1964). Time domain modelling is much more complex since the frequency dependent friction is of fractional order which causes history integrals in time domain descriptions. There, the complex friction behaviour is modelled by some approximation of the inverse Laplace transformation of the wall shear stress (see for instance Zielke (1968)), since exact formulas can't be found.

If frequencies go up into the ranges of several kiloHertz, the spatially one-dimensional transmission line models may loose their validity. Reasons are either that in parts of a transmission line other than axial flow velocities and pressure gradients become significant or that wave propagation phenomena are exhibited by some other fluid filled cavities. In such cases 2D or 3D wave propagation models must be established. Several Finite Element programs (like, e.g., Abaqus and Hibbitt, 2001) offer the modelling and simulation of acoustic fields. But no general purpose programs exist that can simulate viscid wave propagation in fluids with an acceptable efficiency.

The authors have supervised a master's thesis (Furtmüller, 2006) which uses the adaptive Finite Element code hp-FEM (Schöberl, 2006) for the solution of field problems given by partial differential equations to analyse the 3D viscid wave propagation in hydraulic cavities. There, the linearised equations of motion and

This manuscript was received on 20 November 2008 and was accepted after revision for publication on 10 February 2009

continuity of a compressible Newtonian fluid are solved numerically in the frequency domain. High accuracy can be achieved if a fine resolution of the dynamic wall boundary layers in the finite element mesh is done. Since the boundary layer becomes thinner with higher frequencies, different grids should be used for different frequencies in order to avoid unnecessarily high computational effort. The generation of different grids is a drawback for a fast computation of the frequency response behaviour over a large frequency range.

Frequency domain modelling promises to yield the most compact description of the dynamic behaviour of the system. In Manhartsgruber (2005) it was demonstrated how frequency domain models of a transmission line can be combined with time domain computation of nonlinear hydraulic systems by applying Fast Fourier transform and its inverse respectively. Although in this work periodic systems have been investigated there is a realistic perspective to generalise this technique for transient processes. The classical transmission line model was used as a benchmark.

In a thesis by Brummayer (2000) a singular perturbation approach for the viscid wave propagation in lines, originally developed by Kluwick and Gittler (1989) for gas filled tubes, for the computation of viscid wave propagation in hydraulic lines was applied. This work exhibits the physical nature of the friction phenomenon very clearly. The flow in the line consists of a friction dominated dynamic boundary layer which brings all velocity components to zero at the wall of the line and an inviscid flow in the remaining part of the pipe. The inviscid part is affected by friction not by a shear stress but by radial velocity components that are created by the boundary layer and transmitted to the inner parts of the pipe. The results of this approach in terms of the pressure flow rate relations are identical to other results, e.g. D'Souza (1964).

In Scheidl (2006) the dynamic boundary layer theory of Kluwick et al. has been generalised for the 3D case. Starting from the linearised continuity and momentum balance equations for a compressible Newton fluid without bulk viscosity a damped wave equation of the pressure is derived. This equation cannot account for the vanishing fluid velocity at the boundary due to sticking. A boundary layer version of the momentum and continuity relations in frequency domain is derived and matched with the frequency domain version of the wave equation. From these a boundary condition for the pressure is derived.

In this paper the essentials of the theory (Scheidl, 2006) are repeated in a revised form in the next section for an easier understanding and also to show that the pressure boundary condition can be interpreted as a flexible wall with frequency dependent elastic and damping effects. Section 3 explains how this boundary condition can be realised in some standard Finite Element codes within their acoustic modelling framework and how the results compare with the analytical theory of straight transmission lines. In section 4 a useful hydraulic application is shown.

2 A Boundary Layer Theory for 3D Viscid Wave Propagation in Frequency Domain

2.1 Basic Equations of 3D Viscid Linear Wave Propagation

Starting from the linearised equations of motion and continuity in an Eulerian reference frame (Cartesian coordinates (x_1, x_2, x_3)) for a compressible Newtonian fluid with no bulk viscosity as derived, e.g. in Scheidl (2006)

$$\begin{aligned} \dot{\boldsymbol{v}} &= -\frac{1}{\rho_0}\nabla p + \frac{\mu}{\rho_0}\left(\Delta\vec{v} + \tfrac{1}{3}\nabla\left(\nabla\cdot\boldsymbol{v}\right)\right) \\ \frac{\dot{p}}{E} &= -\nabla\cdot\boldsymbol{v} \end{aligned} \tag{1}$$

a viscid wave equation for the pressure can be derived (Scheidl, 2006)

$$\ddot{p} - c^2\Delta p = \tfrac{4}{3}\nu\,\Delta\dot{p}\,,\quad c = \sqrt{\frac{E}{\rho_0}} \tag{2}$$

$\boldsymbol{v}$ is the velocity vector, p the pressure, μ the dynamic viscosity, ρ_0 the density at reference conditions, $\boldsymbol{E}$ the compression modulus, and $\boldsymbol{c}$ the wave propagation speed. But, Eq. 2 only can be solved without Eq. 1 if the pressure or its gradient is given at the whole boundary. This is rarely the case in fluid power applications. The usual condition that the fluid sticks to a solid boundary cannot be accounted for by the pressure only in contrast to the inviscid case where only the velocity component normal to the boundary vanishes. The latter is equivalent to a vanishing pressure gradient in the normal boundary direction. Thus generally, Eq. 2 can only be solved in combination with Eq. 1. Then, however, without a further analysis using Eq. 2 offers no significant advantage.

Of course, Eq. 2 allows the qualitative statement that for a small viscosity ν the effect of the fluid friction on the pressure field is very small in major parts of the fluid domain.

2.2 Nondimensional Equations in Frequency Domain

In the sequel nondimensional values related to the following scales are used.

$$\begin{aligned} &p = \tilde{p}P;\ \boldsymbol{v} = \tilde{\boldsymbol{v}}c\frac{P}{E};\ x_i = \tilde{x}_i L;\ t = \frac{\tau}{\omega}; \\ &\omega = \frac{c}{L};\ \nabla = \frac{1}{L}\tilde{\nabla};\ \varepsilon = \frac{\nu}{cL};\ \frac{\partial}{\partial\tau} = (\ )' \end{aligned} \tag{3}$$

P is a typical pressure amplitude of the wave, L a typical reference length, for instance, the length of a transmission line. This scaling makes both $\tilde{p}$ and $\tilde{\boldsymbol{v}}$ to be of order one. The velocity scale is the so called Joukowski speed.

With the Fourier Transform

$$\hat{p}(f) = \int_{-\infty}^{\infty} \frac{e^{-j\,f\tau}}{\sqrt{2\pi}} \tilde{p}(\tau)\,d\tau;\ \hat{\boldsymbol{v}}(f) = \int_{-\infty}^{\infty} \frac{e^{-j\,f\tau}}{\sqrt{2\pi}} \tilde{\boldsymbol{v}}(\tau)\,d\tau, \quad (4)$$
$$j = \sqrt{-1}$$

Eq. 1 and Eq. 2 take the following form in frequency domain

$$\begin{aligned} j\,f\,\hat{\boldsymbol{v}} &= -\tilde{\nabla}\hat{p} + \varepsilon\left(\tilde{\Delta}\hat{\boldsymbol{v}} + \tfrac{1}{3}\tilde{\nabla}\left(\tilde{\nabla}\cdot\hat{\boldsymbol{v}}\right)\right) \\ j\,f\,\hat{p} &= -\tilde{\nabla}\cdot\hat{\boldsymbol{v}} \end{aligned} \quad (5)$$

$$-f^2\hat{p} - \tilde{\Delta}\hat{p} = j\,f\,\tfrac{4}{3}\varepsilon\tilde{\Delta}\hat{p} \quad (6)$$

ε is a very small quantity in the order of ($10^{-5} \sim 10^{-7}$) for typical values of ν, L, c in hydraulic applications. The terms of Eq. 5 and Eq. 6 with a coefficient ε only can become significant where the velocity or the pressure field have strong local changes. Due to the scaling Eq. 3 the nondimensional wave length is of order 1 for. $f = O(1)$. Local changes only occur at the boundaries due to the vanishing fluid velocity. Thus, Eq. 5 and Eq. 6 are singularly perturbed systems in the parameter ε (see, e.g., Eckhaus (1979), Kevorkian (1980) for singular perturbation theory[1]). The solution is dominated in a larger part of the domain by the reduced equations, which are obtained if the perturbation parameter ε is set to zero. In our case this is the inviscid case. The reduced equations have a reduced order regarding the highest spatial derivative. This does not allow all physical boundary conditions to be fulfilled, in particular the sticking condition. In small zones at the boundaries so called boundary layers occur which locally correct the solutions of the reduced system to fulfil the boundary conditions.

2.3 Matched Asymptotic Expansions of the 3D Viscid Wave Equation

2.3.1 The Outer Expansion

An appropriate set of so called gauge functions (Eckhaus, 1979) of our problem is the sequence $\varepsilon^{k/2}$, k = 0, 1, 2, 3, …. The outer expansion is an asymptotic expansion of the solution outside the boundary layers (the outer range). It is represented here as a series in the gauge functions of the Fourier transform of the pressure and the velocity

$$\begin{aligned} \hat{p}^{ou} &= \hat{p}^{ou}{}_0 + \sqrt{\varepsilon}\,\hat{p}^{ou}{}_1 + \varepsilon\,\hat{p}^{ou}{}_2 + \ldots \\ \hat{v}_i^{ou} &= \hat{v}_i^{ou}{}_0 + \sqrt{\varepsilon}\,\hat{v}_i^{ou}{}_1 + \varepsilon\,\hat{v}_i^{ou}{}_2 + \ldots \quad , \quad i = 1,2,3... \end{aligned} \quad (7)$$

In the outer range the solutions of the reduced equations are a good approximation of the full solution. Furthermore, better solutions can be derived by higher order terms of the asymptotic expansion. For general form of the hydraulic duct in which wave propagation takes place, numerical methods, e.g. the Finite Element method, can be used to obtain approximate solutions. This is not discussed further here. As pointed out in section 2.1 this cannot be done for the pressure wave equation Eq. 1 or Eq. 6 respectively due to missing boundary conditions. To obtain appropriate boundary conditions the boundary layer equations must be solved and matched to the outer solution. This matching provides the boundary conditions for the outer solution.

2.4 The Inner Expansion

At the system's solid boundaries a co-ordinate system $\left(\xi_1^{bl}, \xi_2^{bl}, \xi_3^{bl}\right)$ is used to resolve the boundary layer. The first two axes are tangential the third is perpendicular to the tangent plane, as shown in Fig. 1. We assume that the curvature radii of the boundary as well as the wave length $2\pi c/(f\omega)$ are much larger than the thickness of the boundary layer to avoid cumbersome calculations due to the curved co-ordinate system. Of course, this imposes some restrictions on allowable duct geometries. Edges or a small rounding are not covered by this approach. The question how far such geometric properties adulterate the global behaviour cannot be answered without further investigation. It is doubtful if the linearised equations Eq. 1 are valid there at all. For instance, vortices which are likely to appear there at higher speeds are not in the general solution set of Eq. 1. The normal direction ξ_3 is stretched by $1/\sqrt{\varepsilon}$. This scaling makes the friction term in the momentum equation of equal order of magnitude as the acceleration and pressure gradient terms.

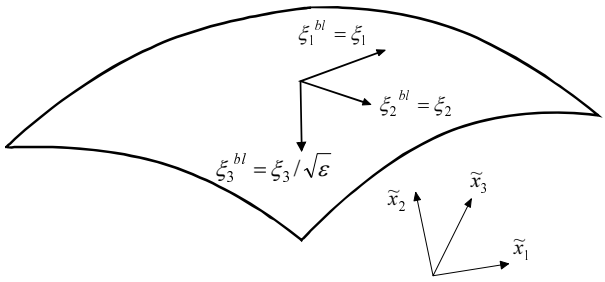

Fig. 1: *Boundary layer co-ordinate system and its scaling*

Expressing Eq. 5 in boundary layer co-ordinates results in the following equations

1 Perturbation methods aim to derive solutions of equations as formal power series in the perturbation parameter ε. For singular perturbation problems which exhibit boundary layers no uniformly valid power series expansion exists. Solutions must be split into an external expansion off the boundary and an inner expansion at the boundary.

$$
j\ \ f\begin{pmatrix}\hat{v}_1^{\,in}\\ \hat{v}_2^{\,in}\\ \hat{v}_3^{\,in}\end{pmatrix}=\begin{pmatrix}-\dfrac{\partial\hat{p}^{in}}{\partial\xi_1^{\,bl}}\\ -\dfrac{\partial\hat{p}^{in}}{\partial\xi_2^{\,bl}}\\ -\dfrac{\partial\hat{p}^{in}}{\sqrt{\varepsilon}\ \partial\xi_3^{\,bl}}\end{pmatrix}+
$$

$$
\varepsilon\begin{pmatrix}\dfrac{\partial^2\hat{v}_1^{\,in}}{\partial\left(\xi_1^{\,bl}\right)^2}+\dfrac{\partial^2\hat{v}_1^{\,in}}{\partial\left(\xi_2^{\,bl}\right)^2}+\dfrac{1}{\varepsilon}\dfrac{\partial^2\hat{v}_1^{\,in}}{\partial\left(\xi_3^{\,bl}\right)^2}\\ \dfrac{\partial^2\hat{v}_2^{\,in}}{\partial\left(\xi_1^{\,bl}\right)^2}+\dfrac{\partial^2\hat{v}_2^{\,in}}{\partial\left(\xi_2^{\,bl}\right)^2}+\dfrac{1}{\varepsilon}\dfrac{\partial^2\hat{v}_2^{\,in}}{\partial\left(\xi_3^{\,bl}\right)^2}\\ \dfrac{\partial^2\hat{v}_3^{\,in}}{\partial\left(\xi_1^{\,bl}\right)^2}+\dfrac{\partial^2\hat{v}_3^{\,in}}{\partial\left(\xi_2^{\,bl}\right)^2}+\dfrac{1}{\varepsilon}\dfrac{\partial^2\hat{v}_3^{\,in}}{\partial\left(\xi_3^{\,bl}\right)^2}\end{pmatrix}+
$$

$$
\frac{\varepsilon}{3}\begin{pmatrix}-\dfrac{\partial}{\partial\xi_1^{\,bl}}\\ -\dfrac{\partial}{\partial\xi_2^{\,bl}}\\ -\dfrac{\partial}{\sqrt{\varepsilon}\ \partial\xi_3^{\,bl}}\end{pmatrix}\left(\frac{\partial\hat{v}_1^{\,in}}{\partial\xi_1^{\,bl}}+\frac{\partial\hat{v}_2^{\,in}}{\partial\xi_2^{\,bl}}+\frac{1}{\sqrt{\varepsilon}}\frac{\partial\hat{v}_3^{\,in}}{\partial\xi_3^{\,bl}}\right)\tag{8}
$$

$$
j\ \ f\ \ \hat{p}=-\left(\frac{\partial\hat{v}_1^{\,in}}{\partial\xi_1^{\,bl}}+\frac{\partial\hat{v}_2^{\,in}}{\partial\xi_2^{\,bl}}+\frac{1}{\sqrt{\varepsilon}}\frac{\partial\hat{v}_3^{\,in}}{\partial\xi_3^{\,bl}}\right)
$$

The solution is represented by an asymptotic expansion

$$
\begin{aligned}&\hat{\mathrm{p}}^{\mathrm{in}}=\hat{\mathrm{p}}^{\mathrm{in}}{}_0+\sqrt{\varepsilon}\hat{\mathrm{p}}^{\mathrm{in}}{}_1+\varepsilon\hat{\mathrm{p}}^{\mathrm{in}}{}_2+\ \ldots\\ &\hat{\mathrm{v}}_{\mathrm{i}}^{\ \mathrm{in}}=\hat{\mathrm{v}}_{\mathrm{i}}^{\ \mathrm{in}}{}_0+\sqrt{\varepsilon}\hat{\mathrm{v}}_{\mathrm{i}}^{\ \mathrm{in}}{}_1+\varepsilon\hat{\mathrm{v}}_{\mathrm{i}}^{\ \mathrm{in}}{}_2+\ \ldots\ \ \mathrm{i}=1,2,3\end{aligned}\tag{9}
$$

Inserting Eq. 9 in Eq. 8 and collecting orders of $\sqrt{\varepsilon}$ results in the following set of equations:

Order $O\left(\varepsilon^0\right)$ and $O\left(\varepsilon^{-1/2}\right)$

$$
\begin{aligned}
j\,f\,\hat{v}_1^{\,in}{}_0&=-\frac{\partial\hat{p}^{in}{}_0}{\partial\xi_1^{\,bl}}+\frac{\partial^2\hat{v}_1^{\,in}{}_0}{\partial\left(\xi_3^{\,bl}\right)^2}\\
j\,f\,\hat{v}_2^{\,in}{}_0&=-\frac{\partial\hat{p}^{in}{}_0}{\partial\xi_2^{\,bl}}+\frac{\partial^2\hat{v}_2^{\,in}{}_0}{\partial\left(\xi_3^{\,bl}\right)^2}\\
j\,f\,\hat{v}_3^{\,in}{}_0&=-\frac{1}{\sqrt{\varepsilon}}\frac{\partial\hat{p}^{in}{}_0}{\partial\xi_3^{\,bl}}+\frac{4}{3}\frac{\partial^2\hat{v}_3^{\,in}{}_0}{\partial\left(\xi_3^{\,bl}\right)^2}-\frac{\partial\hat{p}^{in}{}_1}{\partial\xi_3^{\,bl}}\\
j\,f\,\hat{p}^{in}{}_0&=-\left(\frac{\partial\hat{v}_1^{\,in}{}_0}{\partial\xi_1^{\,bl}}+\frac{\partial\hat{v}_2^{\,in}{}_0}{\partial\xi_2^{\,bl}}+\frac{1}{\sqrt{\varepsilon}}\frac{\partial\hat{v}_3^{\,in}{}_0}{\partial\xi_3^{\,bl}}+\frac{\partial\hat{v}_3^{\,in}{}_1}{\partial\xi_3^{\,bl}}\right)
\end{aligned}\tag{10}
$$

The two terms in the third and fourth equation with a coefficient $1/\sqrt{\varepsilon}$ must vanish to make the asymptotic expansion valid. Thus we have

$$
\frac{\partial\hat{p}^{in}{}_0}{\partial\xi_3^{\,bl}}=0;\ \frac{\partial\hat{v}_3^{\,in}{}_0}{\partial\xi_3^{\,bl}}=0\tag{11}
$$

Since $\hat{v}_3^{\,in}{}_0=0$ at the boundary ($\xi_3^{\,bl}=0$) the second equation in Eq. 11 means that $\hat{v}_3^{\,in}{}_0\equiv 0$.

In other words, the normal fluid velocity in the boundary layer is of order $O\left(\sqrt{\varepsilon}\right)$. This reveals that the lowest order of the asymptotic expansion of the boundary layer solution corresponds to the boundary condition of the inviscid wave equation, namely that the velocity and the pressure gradient in the normal direction vanish. Furthermore, re-evaluating the third equation of Eq. 10 with the last findings yields.

$$
\frac{\partial\hat{p}^{in}{}_1}{\partial\xi_3^{\,bl}}=0\tag{12}
$$

The third equation of Eq. 10 is now fulfilled trivially and does not provide any further information. We have to add the next order (ε^1) of this equation to involve a pressure term, which differs from the solution of the inviscid case.

$$
\begin{aligned}
jf\hat{v}_3^{\,in}{}_1=&-\frac{\partial\hat{p}^{in}{}_2}{\partial\xi_3^{\,bl}}+\tfrac{4}{3}\frac{\partial^2\hat{v}_3^{\,in}{}_1}{\partial\left(\xi_3^{\,bl}\right)^2}\\
&+\tfrac{1}{3}\frac{\partial^2\hat{v}_1^{\,in}{}_0}{\partial\xi_1^{\,bl}\partial\xi_3^{\,bl}}+\tfrac{1}{3}\frac{\partial^2\hat{v}_2^{\,in}{}_0}{\partial\xi_2^{\,bl}\partial\xi_3^{\,bl}}
\end{aligned}\tag{13}
$$

The boundary condition for the inner solution requires that all velocity components vanish at $\xi_3^{\,bl}=0$. At the solid boundaries no pressure can be prescribed. Indeed, the pressure variable $\hat{p}^{in}{}_0$ which is still present in our equations can only be determined by the matching of the inner to the outer expansion (see Section 2.5).

Equations 1,2,4 of Eq. 10 and Eq. 13 can be solved. The solutions are

$$
\begin{aligned}
\hat{v}_1^{\,in}{}_0&=\frac{j}{f}\frac{\partial\hat{p}^{in}{}_0}{\partial\xi_1^{\,bl}}\left(1-e^{\sqrt{f/2}(-1-j)\xi_3^{\,bl}}\right)\\
\hat{v}_2^{\,in}{}_0&=\frac{j}{f}\frac{\partial\hat{p}^{in}{}_0}{\partial\xi_2^{\,bl}}\left(1-e^{\sqrt{f/2}(-1-j)\xi_3^{\,bl}}\right)\\
\hat{v}_3^{\,in}{}_1&=-\sqrt{f/2}\,(1+j)\,\hat{p}^{in}{}_0\left(1-e^{\sqrt{f/2}(-1-j)\xi_3^{\,bl}}\right)\\
\hat{p}^{in}{}_2&=\sqrt{f^3/2}\,(-1+j)\,\hat{p}^{in}{}_0\xi_3^{\,bl}
\end{aligned}\tag{14}
$$

Equation 14 shows that the thickness of the boundary layers is of order $O\left(\sqrt{\varepsilon/f}\right)$ if measured in the outer scale. In physical dimensions the thickness is of order $O\left(\sqrt{\nu/F}\right)$, when F denotes the angular frequency in physical dimensions. The tangential velocity components show up the typical distribution in the normal direction as indicated in Fig. 2. They are 90° phase shifted to the pressure gradient, their amplitude is inversely proportional to the frequency. The normal velocity is of order $O\left(\sqrt{\varepsilon}\right)$, has a distribution in normal direction equivalent to the tangential components, but a quite different frequency dependency and a phase shift of 235° (see Fig. 2). The pressure which is constant in the normal direction in the order ε^0 has a superimposed ε^1 order component $\hat{p}^{in}{}_2$ which causes a linear pressure change in the normal direction.

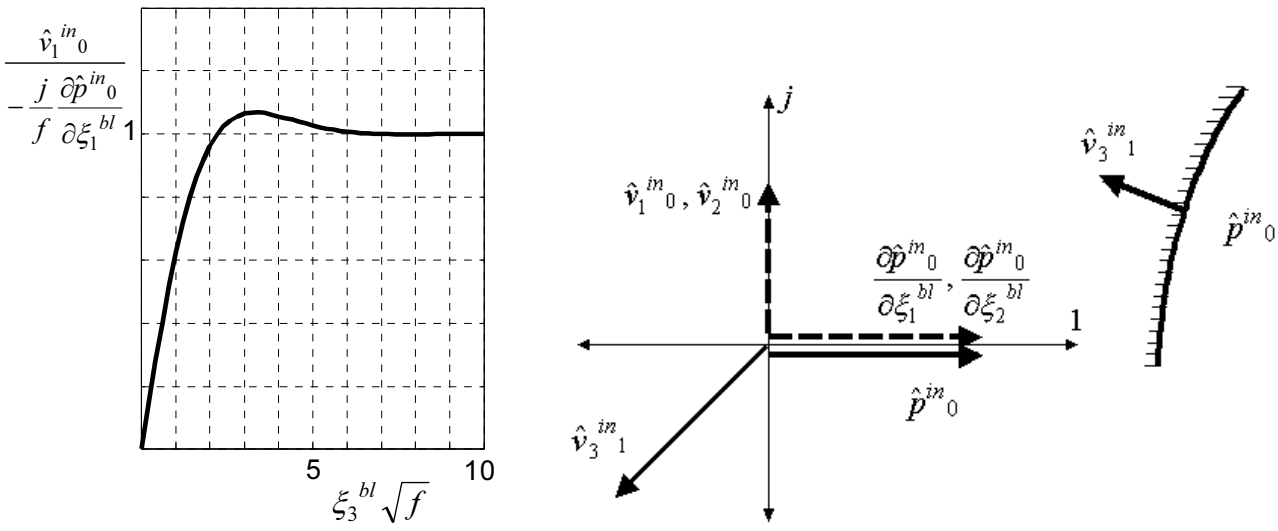

Fig. 2: *Distribution of the nondimensional tangential velocities (scaled by* $-\frac{j}{f}\frac{\partial \hat{p}^{in}{}_0}{\partial \xi_1^{bl}}$*) at the boundary layer according to the inner expansion up to order* ε^0*, phase shift of boundary layer velocities relative to pressure and pressure gradients respectively, and orientation of normal velocity relative to the pressure*

2.5 Matching Inner and Outer Expansions

Inner and outer expansions have to be adapted by a so called matching. Using expansion operators (Eckhaus, 1979) the matching condition for the pressure reads

$$E_{\xi^{bl}}^{(k)} E_{\xi}^{(k)} \hat{p} = E_{\xi^{bl}}^{(k)} E_{\xi}^{(k)} E_{\xi^{bl}}^{(k)} \hat{p}, \quad k = 0, 1, 2, \ldots \tag{15}$$

$E_{\xi}^{(k)} \hat{p} = E^{(k)} \hat{p}^{ou}$ is the outer and $E_{\xi^{bl}}^{(k)} \hat{p} = E^{(k)} \hat{p}^{in}$ is the inner expansion of the pressure series expansion in terms of our gauge functions $\sqrt{\varepsilon}^k$. For $k = 0$, Eq. 15 yields

$$\begin{aligned} &E_{\xi^{bl}}^{(0)} E_{\xi}^{(0)} \hat{p}(\xi_1, \xi_2, \xi_3) = E^{(0)} \hat{p}^{ou}{}_0\left(\xi_1, \xi_2, \sqrt{\varepsilon}\xi_3^{bl}\right) = \\ &\hat{p}^{ou}{}_0(\xi_1, \xi_2, 0) = E_{\xi^{bl}}^{(0)} E_{\xi}^{(0)} E_{\xi^{bl}}^{(0)} \hat{p}\left(\xi_1, \xi_2, \xi_3^{bl}\right) = \\ &E_{\xi^{bl}}^{(0)} E_{\xi}^{(0)} p^{in}{}_0(\xi_1, \xi_2) = \hat{p}^{in}{}_0(\xi_1, \xi_2) \end{aligned} \tag{16}$$

In a similar manner exploiting Eq. 11 and Eq. 12, for $k = 1$ one gets

$$\begin{aligned} E_{\xi^{bl}}^{(1)} E_{\xi}^{(1)} \hat{p}(\xi_1, \xi_2, \xi_3) &= E_{\xi^{bl}}^{(1)}\left(\hat{p}^{ou}{}_0(\xi_1, \xi_2, \xi_3) + \sqrt{\varepsilon}\hat{p}^{ou}{}_1(\xi_1, \xi_2, \xi_3)\right) = \\ &= E^{(1)}\left(\hat{p}^{ou}{}_0\left(\xi_1, \xi_2, \sqrt{\varepsilon}\xi_3^{bl}\right) + \sqrt{\varepsilon}\hat{p}^{ou}{}_1\left(\xi_1, \xi_2, \sqrt{\varepsilon}\xi_3^{bl}\right)\right) = \\ &= \hat{p}^{ou}{}_0(\xi_1, \xi_2, 0) + \sqrt{\varepsilon}\frac{\partial \hat{p}^{ou}{}_0}{\partial \xi_3}(\xi_1, \xi_2, 0)\xi_3^{bl} + \sqrt{\varepsilon}\hat{p}^{ou}{}_1(\xi_1, \xi_2, 0) \\ E_{\xi^{bl}}^{(1)} E_{\xi}^{(1)} E_{\xi^{bl}}^{(1)} \hat{p}\left(\xi_1, \xi_2, \xi_3^{bl}\right) &= E_{\xi^{bl}}^{(1)} E_{\xi}^{(1)}\left(p^{in}{}_0(\xi_1, \xi_2) + \sqrt{\varepsilon}p^{in}{}_1(\xi_1, \xi_2)\right) = \\ &= E_{\xi^{bl}}^{(1)} E_{\xi}^{(1)}\left(p^{in}{}_0(\xi_1, \xi_2) + \sqrt{\varepsilon}p^{in}{}_1(\xi_1, \xi_2)\right) = p^{in}{}_0(\xi_1, \xi_2) + \sqrt{\varepsilon}p^{in}{}_1(\xi_1, \xi_2) \end{aligned} \tag{17}$$

the comparison of which in combination with Eq. 16 leads to

$$\frac{\partial \hat{p}^{ou}{}_0}{\partial \xi_3}(\xi_1, \xi_2, 0) = 0, \quad p^{ou}{}_1(\xi_1, \xi_2, 0) = p^{in}{}_1(\xi_1, \xi_2) \tag{18}$$

For $k = 2$ the matching procedure Eq. 15 results in the following equations

$$\begin{aligned} E_{\xi^{bl}}^{(2)} E_{\xi}^{(2)} \hat{p}(\xi_1, \xi_2, \xi_3) &= \hat{p}^{ou}{}_0(\xi_1, \xi_2, 0) + \varepsilon\tfrac{1}{2}\frac{\partial^2 \hat{p}^{ou}{}_0}{\partial\left(\xi_3^{bl}\right)^2}(\xi_1, \xi_2, 0)\left(\xi_3^{bl}\right)^2 + \varepsilon\frac{\partial \hat{p}^{ou}{}_1}{\partial \xi_3^{bl}}(\xi_1, \xi_2, 0)\xi_3^{bl} + \varepsilon\hat{p}^{ou}{}_2(\xi_1, \xi_2, 0) \\ E_{\xi^{bl}}^{(2)} E_{\xi}^{(2)} E_{\xi^{bl}}^{(2)} \hat{p}(\xi_1, \xi_2, \xi_3) &= E_{\xi^{bl}}^{(2)} E_{\xi}^{(2)}\left(\hat{p}^{ou}{}_0(\xi_1, \xi_2, 0) - \varepsilon\frac{\sqrt{2}}{2}f^{\frac{3}{2}}(1-j)\hat{p}^{in}{}_0(\xi_1, \xi_2)\xi_3^{bl}\right) = \\ &\hat{p}^{ou}{}_0(\xi_1, \xi_2, 0) - \varepsilon\left(\frac{\sqrt{2}}{2}f^{\frac{3}{2}}(1-j)\hat{p}^{in}{}_0(\xi_1, \xi_2)\xi_3^{bl}\right) \end{aligned} \tag{19}$$

Comparing both results of Eq. 19 and inserting identity Eq. 16 yields the wanted boundary condition for the outer expansion of the pressure

$$\frac{\partial \hat{p}^{ou}{}_1}{\partial \xi_3}(\xi_1,\xi_2,0) = -\frac{\sqrt{2}}{2} f^{\frac{3}{2}}(1-j)\hat{p}^{ou}{}_0(\xi_1,\xi_2,0) \qquad (20)$$

Additionally, we get

$$\frac{\partial^2 \hat{p}^{ou}{}_0}{\partial(\xi_3)^2}(\xi_1,\xi_2,0) = 0, \quad \hat{p}^{ou}{}_2(\xi_1,\xi_2,0) = 0 \qquad (21)$$

2.6 Dynamical Boundary Layer as a Flexible Wall

Due to the momentum equation Eq. 5 the pressure gradient in normal direction equals the normal velocity time derivative $\frac{\partial \hat{p}^{ou}{}_1}{\partial \xi_3} = -j f \hat{v}_3{}^{ou}{}_1$. Inserting this in Eq. 20 and transforming to physical quantities we get the following relation of first order (up to $\sqrt{\varepsilon}$) validity

$$\bar{v}_3 = -\bar{p}\frac{\sqrt{2\nu F}}{2E}(1+j) + O(\varepsilon) \qquad (22)$$

$\bar{v}_3$, $\bar{p}$ are the Fourier transformed normal velocity and pressure, respectively. F is the angular frequency used in the Fourier Transform in physical dimensions. Equation 22 has an intuitive mechanical interpretation that refers directly to typical acoustical boundary settings. Note that the ξ_3- coordinate of the local coordinate system is oriented inwards, hence also a positive velocity component $\bar{v}_3$. The complex coefficient $\frac{\sqrt{2\nu F}}{2E}(1+j)$ is the acoustic admittance. It represents elastic and damping behaviour, the latter, of course, is responsible for the dissipation of the viscous effects in the dynamic boundary layer. A usual notation that is for instance applied in the acoustic modelling framework of the Finite Element program Abaqus reads in time and frequency domain

$$\begin{aligned} \dot{u}_{out} &= \frac{1}{k_1}\dot{p} + \frac{1}{c_1}p \\ \bar{v}_{out} &= \left(jF\frac{1}{k_1} + \frac{1}{c_1}\right)\bar{p} \end{aligned} \qquad (23)$$

u_{out}, v_{out} are the outward displacement and velocity respectively at the boundary. In mechanical terms k_1 is an elastic stiffness and c_1 a damping coefficient or, in other words, the coefficients of a frequency dependent visco-elastic boundary. This property is sketched in Fig. ***3***.

Comparing Eq. 22 with Eq. 23 results in the following equations for k_1 and c_1

$$c_1 = -\frac{E\sqrt{2}}{\sqrt{\nu F}}\ ;\ k_1 = -\frac{E\sqrt{2F}}{\sqrt{\nu}} \qquad (24)$$

Of course this result is not valid for very low frequencies F since then $1/k_1$ tends to grow to infinity. The physical reason behind that breakdown of this approach at low frequencies is that the boundary layer thickness which is of order $O\left(\sqrt{\nu/F}\right)$ is growing to infinity but is unaffected by other boundary layers whereas in reality layers of opposite sides will interact. For pipe flow, for instance, the very low frequency situation is described by the well know Hagen-Poiseuille parabolic profile. The boundary layer thickness for a typical hydraulic oil with 46 mm^2/s kinematic viscosity and a frequency of 10 Hz ($F = 20\pi/s$) is estimated to be approximately 6 mm if we conclude from Fig. 2 that the nondimensional layer thickness is about 6.

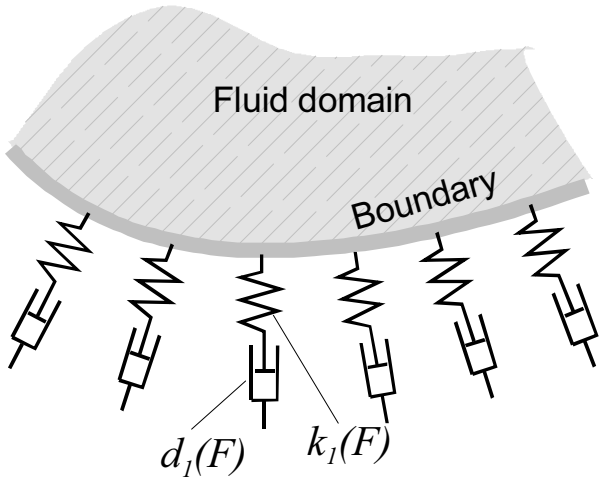

Fig. 3: *Frequency dependent visco-elastic boundary condition as a mechanical equivalent of the viscous boundary layer*

3 Finite Element Analysis of Viscid Waves

The results of the last section in combination with the wave equation Eq. 2 and the estimate given in section 2.2 for the nondimensional viscosity value ε suggest the following procedure to compute wave propagation problems in 3D.

- Use acoustic frequency domain finite elements for describing the behaviour in the domain of the fluid apart from the boundary layer. In the terminology of singular perturbation theory this is the zero order term of the outer expansion or a solution of the reduced problem which is the inviscid wave equation Eq. 2 with $\varepsilon = 0$.
- Apply frequency dependent acoustic boundary conditions according to Eq. 23.

3.1 Realization in the Finite Element System Abaqus

The Abaqus finite element system (Hibbit, 2001) can run a linear acoustic analysis including also the coupling of acoustic fields with elastic structures. For this purpose, different acoustic elements from 1D to 3D and axisymmetric cases are available. Different boundary conditions: stiff boundary, prescribed pressure,

coupling with a mechanical structure, frequency dependent impedance boundary also coupled to a mechanical structure, and radiating boundaries for exterior problems and distributed loads in form of a volumetric acceleration, can be modelled.

Concerning the procedures for acoustic analysis the *Steady State Dynamics* analysis of Abaqus is relevant for this frequency domain wave propagation method, because the *Direct Time Integration* cannot model frequency dependent impedance boundary conditions.

3.2 Benchmark Example Straight Circular Pipe

For an easy comprehension and for a verification the example of a straight, circular, rigid pipe closed at its left end and with a prescribed periodic pressure at its right end is treated. The FE mesh and the boundary conditions are indicated in Fig. 4. Further data of this model can be found in the partial listing of the corresponding Abaqus input file in the Appendix. The visco-elastic boundary conditions have to be applied at all closed surfaces, in this example in principle also at the left side end surface, even though this has no significant influence on the results. If, however, the diameter to length ratio becomes much larger the dynamical boundary layer friction at the end surface has substantial influence on the system behaviour.

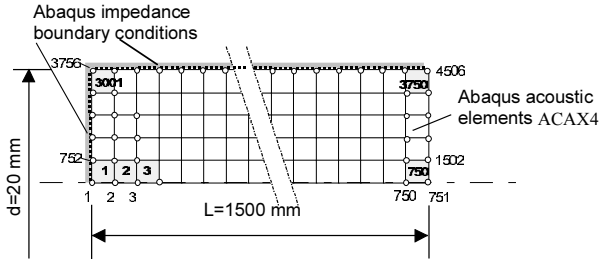

Fig. 4: *Axisymmetric FE model of a hydraulic wave in a straight pipe*

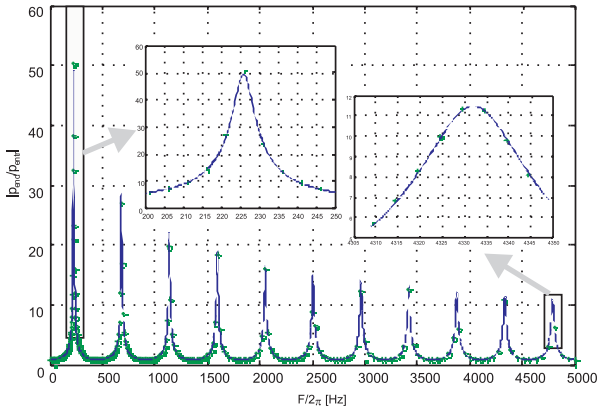

Fig. 5: *Amplitude of frequency response of the closed end pressure p_{end} to input pressure p_{entr} ratio (+) and corresponding value of the analytical theory of D'Souza (1964) (—)*

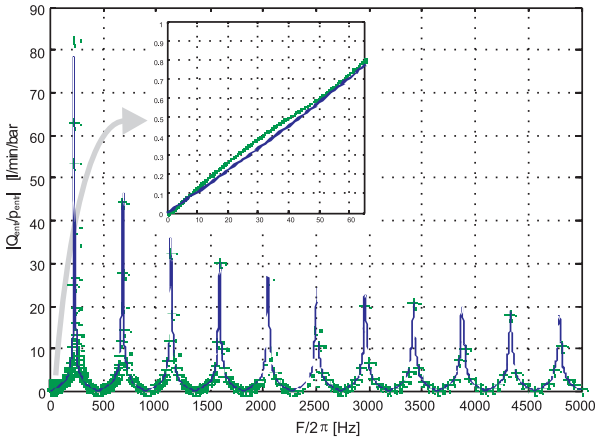

Fig. 6: *Amplitude of frequency response of the input flow rate Q_{entr} to input pressure p_{entr} ratio (+) and corresponding value of the analytical theory of D'Souza (1964) (—)*

The applied *Steady State Dynamics, Direct* procedure of Abaqus generates a frequency sweep which generates directly the frequency response behaviour of the system to the applied input load, in this case the periodic pressure oscillation at the open end of the pipe. The results of this computation are shown in Fig. 5 and Fig. 6 and are compared with the well known theory of D'Souza (1964). The agreement is excellent even down to rather low frequencies. The practical validity range concerning the low frequency limit is even better than the estimate for a circular pipe of section 2.6. The practical reason for that becomes apparent if one looks to the values of the admittance $1/k_1$ of the Abaqus input file in the Appendix. Even for the lowest investigated frequency of 0.01 Hz it is still a rather small value and the singularity for $F \rightarrow 0$ according to Eq. 1 becomes striking only for much smaller values of F.

3.3 Example: Transfer behaviour of curved pipes

The transfer behaviour of curved pipes in the linear acoustic validity range can be studied by this method. In Fig. 7 a result obtained by Abaqus in terms of the acoustic velocity field amplitudes for the indicated frequency of 102 Hz is shown for a doubly coiled pipe with a circular cross section. An excitation amplitude of 50 bar is applied at the lower end and no pressure oscillation at the upper end of the coil. The inner parts show larger velocities than the outer parts. The respective transfer behaviour is compared in Fig. 8 with those of the straight pipe and a semicircle pipe both having the same centre line length (1.5 m) and diameter (40 mm) in the neighbourhood of a resonance frequency. All three FE models have a similar grid size of the FE mesh. To show that the FE model of the straight pipe is quite accurate in this frequency range also the analytical results of D Souza's theory are included. There is only a small shift in the resonance frequency and a bit more damping.

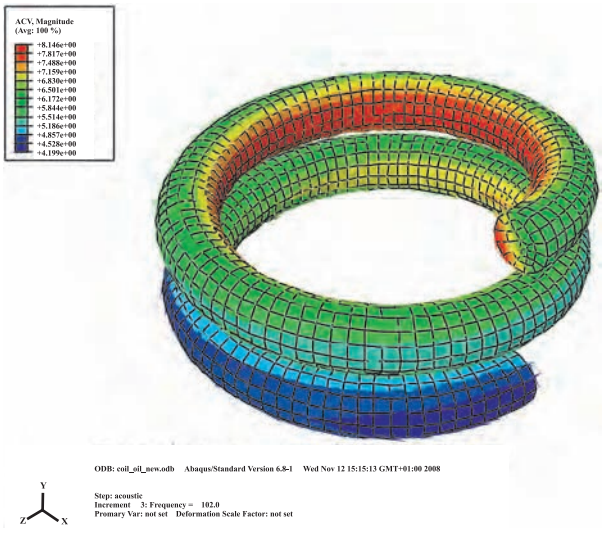

Fig. 7: *Acoustic velocity amplitudes in the pipe coil at excitation frequency 102 Hz.*

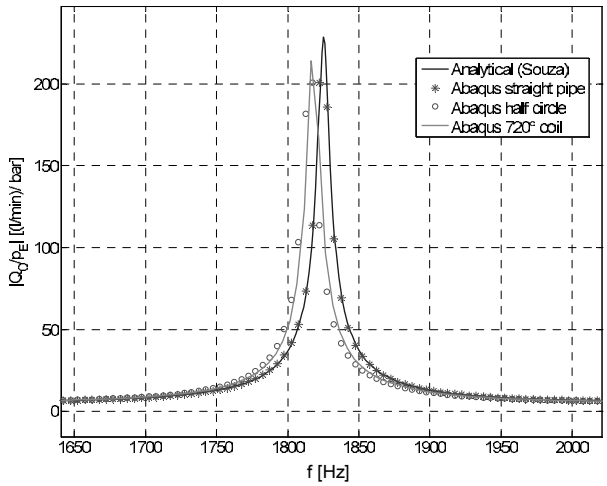

Fig. 8: *Spectrum Amplitude response of the outlet flow rate Q_O (upper coil end) versus of input pressure p_E near a resonance point for different models and pipe curvatures*

It must be pointed out that the linear acoustic equations Eq. 1 do not include the convective acceleration term and cannot create effects like the formation of vortices or vortex shedding. Such effects are typically encountered already for stationary or low frequency oscillating incompressible flow conditions and have significant influence on flow resistance. An open question is what effect fluid compressibility has on these or similar phenomena.

4 Conclusion and Outlook

The dynamical boundary layer theory of viscid wave propagation opens the door to simulate 3D viscid wave propagation with standard inviscid acoustic FE-models if these models are endowed with frequency dependent boundary impedance. The validity of this approach was demonstrated by a comparison with analytical results for the circular straight pipe. The practical use of this modelling technique was shown for a pipe coil.

This frequency domain based method can be exploited also for time domain simulations. A method which is based on Fast Fourier Transform can be found in Manhartsgruber (2005). Methods to approximate the frequency domain transfer behaviour by linear state space models as discussed in Manhartsgruber (2005), Manhartsgruber (2006) can also be applied.

The method for computing 3D viscid wave propagation will be used frequently for the investigation of specific hydraulic systems. Major fields will be hydraulic switching converters, attenuation devices, and other systems in which fast hydraulic processes generate wave propagation effects with a significant 3D characteristics in part of the hydraulic pathway.

Of course, this theory is limited to the linearised wave equation. Effects due to the convective acceleration term or due to a nonlinear compressibility law, for instance resulting from entrapped air or a cavitating fluid, are not included in this approach and cannot be covered by frequency domain methods. The modelling and experimental investigation of such type of wave propagation phenomena will be studied more intensively in the future with direct CFD simulations and with experiments. It is planned to apply OpenFoam open source software [OpenFOAM®] and to use a flexible, match-box type test rig developed at the authors' institute for wave propagation experiments of different geometries.

Typical computing times of 3D CFD hydraulic wave simulations as communicated by the Hydraulic Systems Design Research Group at the Engineering Sciences and Methods Department of the University of Modena and Reggio Emilia are in the range of many hours or even days, compared to only minutes for our approach. This computational advantage is essential for extensive design studies and optimizations.

Since in general linear methods are part of solution procedures of nonlinear problems, the method presented in this paper may be helpful also as an efficient linear solver for nonlinear wave propagation problems.

Nomenclature

c	Wave propagation speed	[m/s]
c_1	Damping coefficient of mechanical boundary layer model	[kg/(m^{2}s)]
E	Fluid compression modulus	[bar]
$E_{\xi}^{(k)}$	Expansion operators for outer co-ordinates	
$E_{\xi^H}^{(k)}$	Expansion operators for inner co-ordinates	
f	Nondimensional angular frequency	
F	Physical angular frequency	[rad/s]
$\vec{\vec{I}}$	Identity tensor	
j	Imaginary unit	
k_1	Elastic stiffness of mechanical boundary layer model	[kg/(m^{2}s^2)]

L	Length scale for nondimensionalisation	[m]
p	Physical pressures	[bar]
$\widetilde{p}$	Nondimensional pressure	
Δ	Laplacian operator	[1/m^2]
∇	Nabla operator	[1/m]
$\widetilde{\Delta}$, $\widetilde{\nabla}$	Nondimensional Δ, ∇	
ε	Nondimensional friction parameter	
μ	Dynamic viscosity of fluid	[Pa s]
$\nu = \frac{\mu}{\rho_0}$	Kinematic viscosity of fluid	[mm^2/s]
$\hat{p}$	Fourier Transform of $\widetilde{p}$	
$\hat{p}^{in}{}_k$	Term of order k of the inner asymptotic expansion of $\hat{p}$	
$\hat{p}^{ou}{}_k$	Term of order k of the outer asymptotic expansion of $\hat{p}$	
P	Pressure scale for nondimensionalisation	[bar]
$\boldsymbol{v}$	Fluid velocity vector	[m/s]
$\widetilde{\boldsymbol{v}}$	Nondimensional fluid velocity vector	
$\hat{v}_i, i = 1...3$	i-th component of the Fourier Transform of $\widetilde{\boldsymbol{v}}$	
$x_i, i = 1..3$	Co-ordinates	[m]
$\widetilde{x}_i, i = 1..3$	Nondimensional coordinates	
ρ	Fluid density	[kg/m^3]
ρ_0	Fluid density reference value at zero pressure	[kg/m^3]
τ	Nondimensional time	
ω	Scaling frequency	[rad/s]
$\xi_i, i = 1..3$	Nondimensional co-ordinates at the boundary	
$\xi_i^{bl}, i = 1..3$	Nondimenional co-ordinates for the boundary layer	

Acknowledgement

This work has been sponsored by the Austrian Center of Competence in Mechatronics (ACCM) which is a COMET K2 center and is funded by the Austrian Federal Government, the Federal State Upper Austria, and its Scientific Partners.

References

Brummayer, M. 2000. *Wellenausbreitungsvorgänge in hydraulischen Wellenkonvertern unter Berücksichtigung von Reibungseffekten*. Doctoral thesis. Johannes Kepler University Linz.

D'Souza, A. and **Oldenburger, R.** 1964. Dynamic Response of Fluid Lines. *Trans. ASME, Journal Basic Engng*, 86, pp. 589-598.

Eckhaus, W. 1979. *Asymptotic Analysis of Singular Perturbations*. North- Holland.

Furtmüller, J. 2006. *Berechnung einer Rohrströmung mit der Methode der Finiten Elemente und Vergleich mit analytischen Lösungen*. Master's thesis. Johannes Kepler University Linz.

Gittler, Ph. and **Kluwick, A.** 1989. Dispersive Wandreibungseffekte bei hochfrequenten Wellen in gasgefüllten Rohren. *ZAMM* 69, 578-579.

Hibbit, Karlsson and **Soresnsen, Inc.** 2001. *Abaqus/Standard User's Manual*, Version 6.2.

Kevorkian, J. and **Cole, J.D.** 1980. Perturbation Methods in Applied Mathematics. Series: *Applied Mathematical Sciences*, Vol. 43, Springer.

Manhartsgruber, B., **Mikota, G.** and **Scheidl, R.** 2005. Modelling of a Switching Control Hydraulic System. *Mathematical and Computer Modelling of Dynamical Systems*, 11, pp. 329-344.

Manhartsgruber, B. 2005. Reduced Order, Discrete-Time, Input-Output Modelling of Laminar Pipe Flow. *WSEAS, in IASME Transactions* Vol. 2, No. 6, pp. 911-18.

Manhartsgruber, B. 2006. On the Passivity of a Galerkin Finite Element Model For Transient Flow in Hydraulic Pipelines. *Proceedings of the Institution of Mechanical Engineers, Part I: Journal of Systems and Control Eng.* Vol. 220, No. 3, pp. 223-237.

OpenFOAM®, http://www.opencfd.co.uk/openfoam

Scheidl, R. and **Manharstgruber B.** 2006. On 3D viscid periodic wave propagation in hydraulic systems, *Power Transmission and Motion Control - PTMC* 2006. pp. 109-120.

Schöberl, J. 2006. Start Project: 3D hp-Finite Elements: Fast Solvers and Adaptivity. Sponsored by the Austrian Science Foundation (FWF), http://www.hpfem.jku.at/index.html?/joachim/ (March).

Stecki, J. and **Davis, D.** 1986. Fluid Transmission Lines – Distributed Parameter Models. Part1: A review on the State of the Art. *Proc. Instn. Mech. Engnrs. Part A*, 200, pp. 215-228.

Zielke, W. 1968. Frequency-Dependent Friction in Transient Pipe Flow. *Trans. ASME, Journal Basic Engng.*, 90, pp. 109-115.

Appendix 1

ABAQUS input file for example section 3.2

```
*Heading
** Job name: Frequency response straight line; Length: 1.5 m; diameter: 20 mm; Abaqus Version 6.6
*Preprint, echo=NO, model=NO, history=NO, contact=NO
**
** PARTS
**
*Part, name=Fluid
** Define the nodes of the mesh
*Node
      1,          0.,         1.5
      2,          0.,   1.49800014
      3,          0.,   1.49599993
…
  4505, 0.00999999978, 0.00200000009
  4506, 0.00999999978,          0.
** Define the elements: Abaqus acoustic 4 node element: ACAX4
*Element, type=ACAX4
  1,  1,  2,  753,  752
  2,  2,  3,  754,  753
…
3749, 3753, 3754, 4505, 4504
3750, 3754, 3755, 4506, 4505
** Define Node-sets and Element-sets
*Nset, nset=Fluid, generate
  1,  4506,    1
*Elset, elset=Fluid, generate
  1,  3750,    1
** Section: Fluid: Define fluid properties, by referring to the material 'oil' for all fluid elements
*Solid Section, elset=Fluid, material=oil
1.,
*End Part
** ASSEMBLY
*Assembly, name=Assembly
**
*Instance, name=Fluid-1, part=Fluid
*End Instance
** Define further Node- and Element-sets for load and boundary definitions
*Nset, nset=acoustic_pressure,internal, instance=Fluid-1,generate
  751,  4506,   751
*Elset, elset=acoustic_pressure, internal, instance=Fluid-1,generate
  750,  3750,   750
*Elset, elset=boundary_layer_admittance_S3, internal, instance=Fluid-1, generate
 3001,  3750,    1
*Elset, elset=boundary_layer_admittance_S4, internal, instance=Fluid-1, generate
  1,  3001,   750
*Surface, type=ELEMENT, name=boundary_layer_admittance
boundary_layer_admittance_S3, S3
boundary_layer_admittance_S4, S4
*End Assembly
**
** MATERIALS
** Define compression modulus and deinsity of the fluid
*Material, name=oil
*Acoustic Medium
 1.6e+09,
*Density
850.,
**
** INTERACTION PROPERTIES
** The first column is the values of '1/k' the real part =sqrt( ν F/2(E*ω)
**The second column is the values of '1/ c' the imaginary part = sqrt( ν F/2)/E
** The third column is the frequency F/(2π)
*Impedance Property, name=boundary_layer_admittance
 1.1958e-11, 7.5134e-13,       0.01
 3.7814e-12, 2.3759e-12,        0.1
   1.2e-12,   7.51e-12,         1.
  1.69e-13,   5.31e-11,        50.
   1.2e-13,   7.51e-11,       100.
…
  1.71e-14,   5.26e-10,      4900.
   1.7e-14,   5.29e-10,      4950.
  1.69e-14,   5.31e-10,      5000.
**
**
*Acoustic Wave Formulation, type=TOTAL WAVE
** ----------------------------------------------------------
** Tjis defines the calculation procedure
** STEP: acoustic
**
*Step, name=acoustic, perturbation
Frequency_response
*Steady State Dynamics, direct
0.01, 5000., 1000, 1.
**
** BOUNDARY CONDITIONS
** This defines the load: input pressure amplitude of 50 bar (5e6 Pascal); only a real part is
** taken!
** Name: acoustic_pressure Type: Acoustic pressure
*Boundary, load case=1
acoustic_pressure, 8, 8, 5e+06
*Boundary, load case=2
acoustic_pressure, 8, 8
**
** INTERACTIONS
** This defines the acoustic boundary conditions by which the viscous boundary layer is
** modeled
** Interaction: admittance
*Simpedance, property=boundary_layer_admittance
boundary_layer_admittance
**
** OUTPUT REQUESTS
```

```
**
** FIELD OUTPUT: F-Output-1
**
*Output, field
*Node Output
POR
*Element Output, directions=YES
ACV
**
** HISTORY OUTPUT: H-Output-1
**
*Output, history, variable=PRESELECT
*End Step
```


Rudolf Scheidl
Dipl.-Ing., Dr., Professor of Mechanical Engineering at Mechatronics Department of Johannes Kepler University Linz. Head of the Institute of Machine Design and Hydraulic Drives. Masters and doctoral degree from Vienna University of Technology. R&D positions in agricultural, steel and paper production machine building industry. Main research interests in fast hydraulic processes, hydraulic switching control, and mechatronic design.

Bernhard Manhartsgruber
Dipl.-Ing., Dr., Associated Professor at the Institute of Machine Design and Hydraulic Drives, Johannes Kepler University, Linz, Austria. Masters and doctoral degree from Johannes Kepler University. Habilitation for Machine Design and Hydraulic Drives in 2005. Main research interests in modelling and simulation of fluid power systems, especially with wave propagation in fast hydraulic systems.

Mohamed Ez El Din
BSc and MSc in Automotive and Tractors Engineering, Helwan Universtiy, Cairo, Egypt. His current PhD thesis on modelling and simulation of hydraulic accumulator and compensator technologies at Johannes Kepler University Linz are sponsored by a scholarship form the ÖAD (Austrian Exchange Service).